CHAPTER 4

4. RESULTS AND DISCUSSION

4.1. Characterization of TiO_2 photocatalyst

4.1.1. Characterization by X-ray diffraction.

The XRD analysis of the TiO_2 sample was done using SCHIMADZU (Japan) make diffractometer using Cu-Kα X-rays of wavelength (λ)=1.5406 Å. The pattern was collected in the range of 4-140° 2θ with a scan step of 0.02 in a continuous scan mode.

The X-ray diffraction pattern of the Titania sample is shown in Figure 4.1. The absence of spurious diffractions indicates the crystallographic purity. The experimental XRD pattern agrees with the JCPDS card no. 21-1272 (anatase TiO_2) and the XRD pattern of TiO_2 nanoparticles other literature. The Strong diffraction peaks at 25.27° and 48.01° indicating TiO_2 in the anatase phase. The intensity of XRD peaks of the sample reflects that the formed nanoparticles are crystalline and broad diffraction peaks indicate very small size crystallite[126, 96]. From this study, considering the peak at degrees, average particle size has been estimated by using Debye-Scherer formula. Inter-planar spacing between atoms (d-spacing) is calculated using Bragg's Law

$$\mathbf{D = \frac{0.9\,\lambda}{\beta \cos \theta}}$$

$$\mathbf{2\,d \sin\theta = n\lambda}$$

Where,

λ is wave length of X-Ray (0.1540 nm),

β is FWHM (full width at half maximum),

θ is diffraction angle,

d is inter-planer spacing

D is particle diameter size.

In order to find β, the full-width of the peak was calculated at half maxima of X-ray diffraction peaks. The results were obtained after the instrument was corrected. The mean crystallite size of the researched photocatalyst calculated from the discussed method was found to be in the range of 75-81 nm.

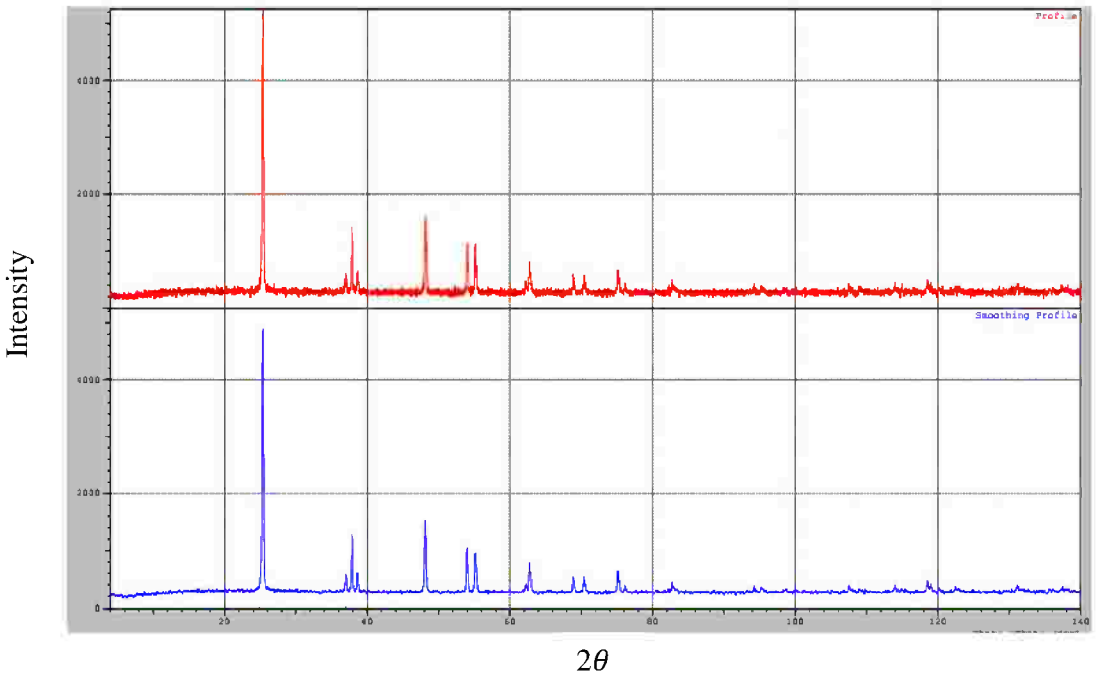

Figure 4.1: XRD pattern of TiO_2 semiconductor

4.1.2. Characterization by particle size analyzer

The particle size analysis of the TiO_2 sample was done using N5 Submicron particle size analyzer, BeckMan Coulter using water as diluent at different to angles 11^o and 90^o. The particle size pattern of the Titania sample is shown in Figure 4.2. The mean particle size of titanium dioxide was found to be in the nanosize ranging from 14.9 nm at angle of 11^o and 192.5 nm at 90^o as shown in table 4.1

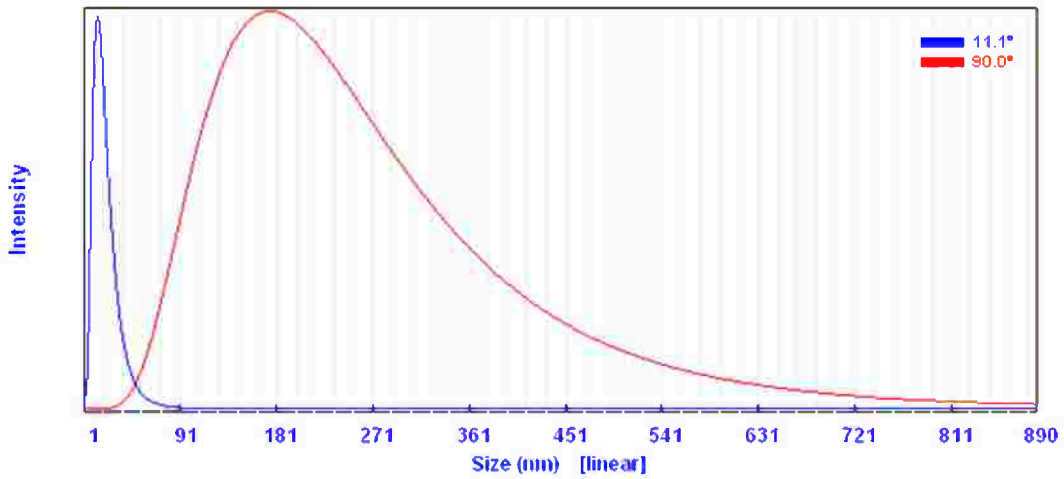

Figure 4.2: Particle size pattern of TiO_2 at two different angles

Table 4.1 Unimodal results summary of TiO_2 at two different angles

Angle	Mean (nm)	P.I.	Diff.Coef (m^2/s)	Counts/s	Baseline Error	Overflow
11.1°	14.9	0.987	2.87e-11	1.06e+06	0.03%	0
90.0°	192.5	0.780	2.22e-12	1.61e+06	0.01%	0

4.1.3. Characterization by scanning electron microscope

The scanning electron microscopic (SEM) is the primary tool uses for characterization of the surface morphology and fundamental physical properties of photocatalyst surface. It is useful for determining the particle size, shape, porosity, and appropriate size distribution of the TiO_2. The SEM photograph was recorded by using JOEL Japan, (Model JSM-636OLA,). Scanning electron image of TiO_2 powder shows that the particles appears in spherical form(figure 4.3).also, before and after the experiment, SEM images of the immobilized TiO_2 on glass substrate was detected (figure 4.4, 4.5). The SEM photographs show that particles are spherical with size ranging from 120-180 nm. The surface texture was found rough.

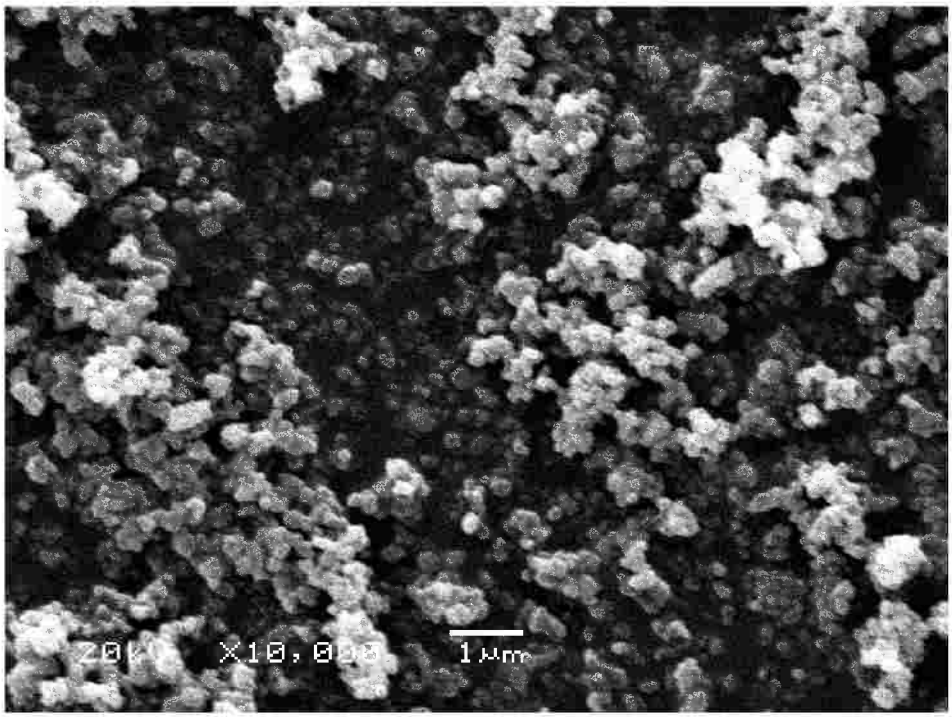

Figure 4.3: SEM image of TiO_2 photocatalyst at 10000 x

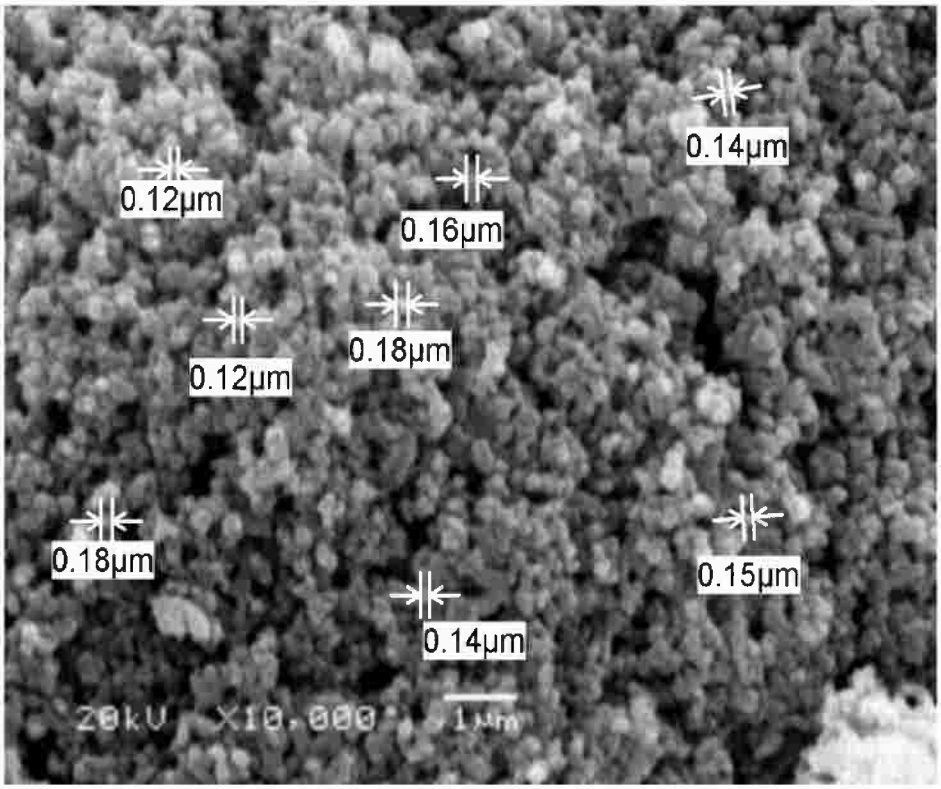

Figure 4.4: SEM image of immobilized TiO_2 photocatalyst at 10000 x before experiment

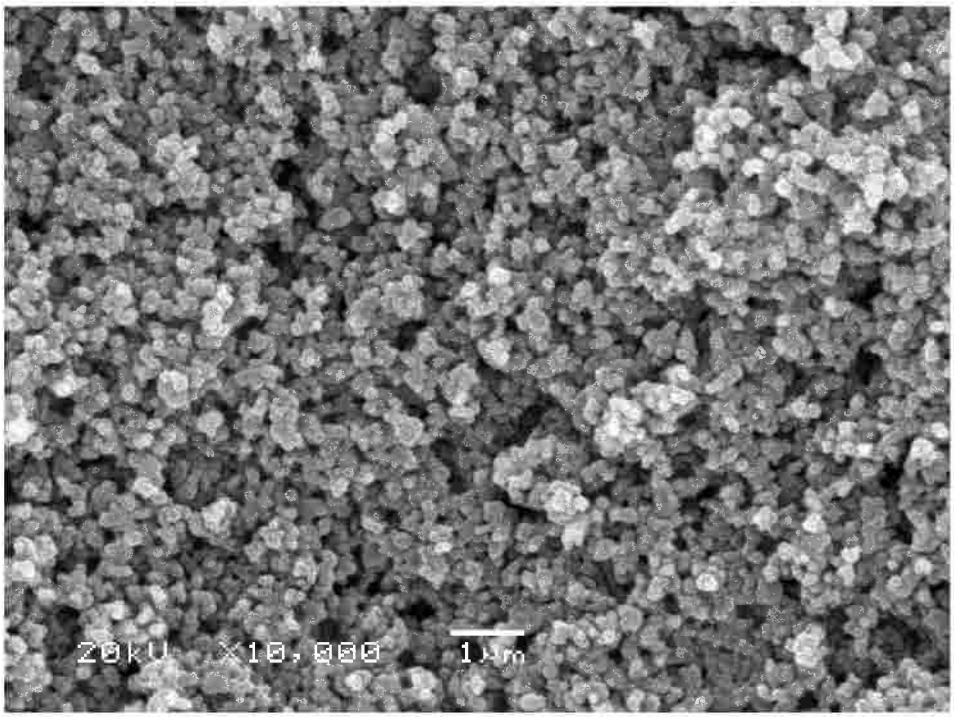

Figure 4.5: SEM image of immobilized TiO_2 photocatalyst at 10000 x after experiment

4.2. Photocatalytic degradation of methylene blue

The degradation of methylene blue is carried out in the presence of UV/titania system. TiO_2 is activated by absorption of a photon with sufficient energy (equals or higher than the band-gap energy (E_{bg}) of the catalyst). The absorption leads to a charge separation due to promotion of an electron (e^-) from the valence band of the semiconductor catalyst to the conduction band, thus generating a hole (h^+) in the valence band. The photogenerated electrons could reduce the dye or react with electron acceptors such as O_2 adsorbed on the Ti (III)-surface or dissolved in water, reducing it to superoxide radical anion $O_2^{-\bullet}$. The photogenerated holes can oxidize the organic molecule to form R^+, or react with OH^- or H_2O oxidizing them into $OH^\bullet$ radicals. Together with other highly oxidant species (peroxide radicals) they are reported to be responsible for the heterogeneous TiO_2 photodecomposition of organic substrates as dyes. The resulting $OH^\bullet$ radical, being a very strong oxidizing agent (standard redox potential +2.8 V) can oxidize most dyes to the mineral end-products. According to this, the relevant reactions at the semiconductor surface causing the degradation of dyes can be expressed as follows:[4]

$TiO_2 + hv\ (UV) \rightarrow TiO_2\ (e_{CB-} + h_{VB+})$

$TiO_2\ (h_{VB+}) + H_2O \rightarrow TiO_2 + H^+ + OH^\bullet$

$TiO_2\ (h_{VB+}) + OH^- \rightarrow TiO_2 + OH^\bullet$

$TiO_2\ (e_{CB-}) + O_2 \rightarrow TiO_2 + O_2^{\bullet-}$

$O_2^{\bullet-} + H^+ \rightarrow HO_2^\bullet$

$2HO_2^\bullet \rightarrow H_2O_2 + O_2$

$H_2O_2 + e^- \rightarrow OH^- + OH^\bullet$

$Dye + OH^\bullet \rightarrow$ degradation products

$Dye + h_{VB+} \rightarrow$ oxidation products

In the present case, photo-holes are certainly not concerned by the initial step since the reactant is cationic and not electron donor. By contrast, the $OH^\bullet$ radicals can attack the $C–S^+=C$ functional group in MB. Therefore, the initial step of MB degradation can be ascribed to the cleavage of the bonds of the $C–S^+=C$ functional group in MB[110].

4.2.1. Effect of initial solution pH

Because of the amphoteric behaviour of most semiconductor oxides, an important parameter governing the rate of reaction taking place on semiconductor particle surfaces is the pH of the dispersions, since; it influences the surface-charge-properties of the photocatalysts. Further, industrial effluents may not be neutral. Therefore, the effect of initial solution pH on the rate of degradation needs to be considered. To study the effect of pH on the decolorization of dye, experiments were carried out at three pH values namely 3, 5 and 7. The effect of initial solution pH on the degradation percent of the dye is shown in figures (4.6-4.10). In agreement with previous studies, the percentage degradation of the dye increases with increasing the pH from 3 to 7 [114, 110, 109, 112]. The pH effect can be explained on the basis of the zero point of charge of TiO_2. The adsorption of H_2O molecules at surface metal sites is followed by the dissociation of the OH groups leading to the coverage with chemically equivalent metal hydroxides (TiOH). Due to the amphoteric behavior of TiO_2, the following equilibrium reactions should be considered.

$$TiOH + H^+ \rightarrow TiOH_2^+ \qquad pH < pH\ zc$$

$$TiOH + OH^- \rightarrow TiO^- + H_2O \qquad pH > pH\ zc$$

The changes in pH value can thus influence the adsorption of molecules onto the TiO_2 surface, an important step for the photo-oxidation to take place. For the TiO_2 sample used zero point charge (pH zc) is around 5.8 to 6.8 [127]. As a consequence of this amphoteric behavior the titanium oxide surface is predominantly positively charged below pH zc and negatively charged above. So when pH is more than 6 a strong adsorption of positively charged MB on the TiO_2 particles occurs as a result of the attraction of the negatively charged TiO_2 with the positively charged dye. In this case, the highest decolorization percentage was achieved at pH 7 [128].

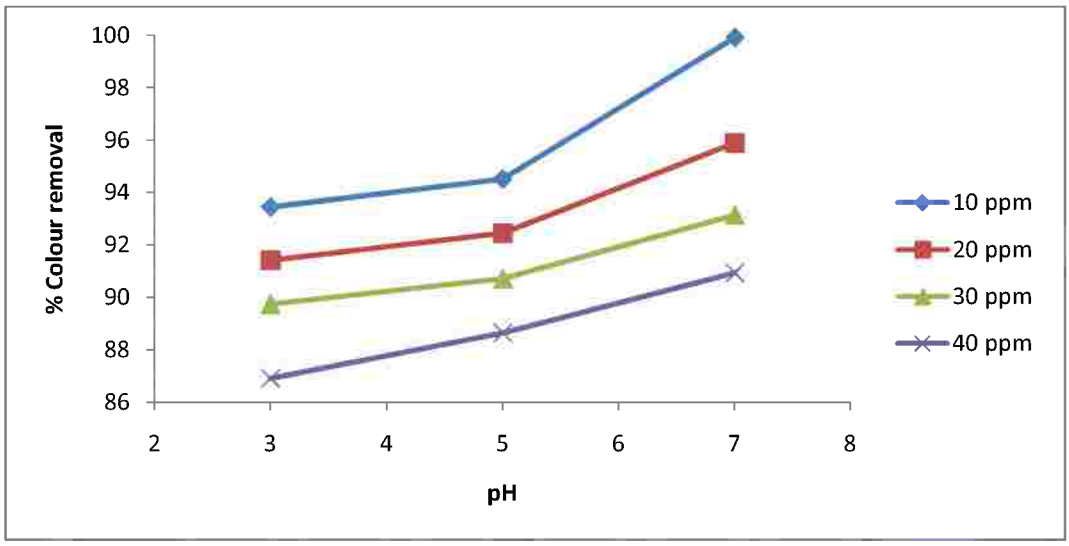

Figure 4.6: Effect of pH on the percentage colour removal of MB at different initial dye concentration (Catalyst loading = 1 g/l, air superficial velocity = 1.94 cm/s)

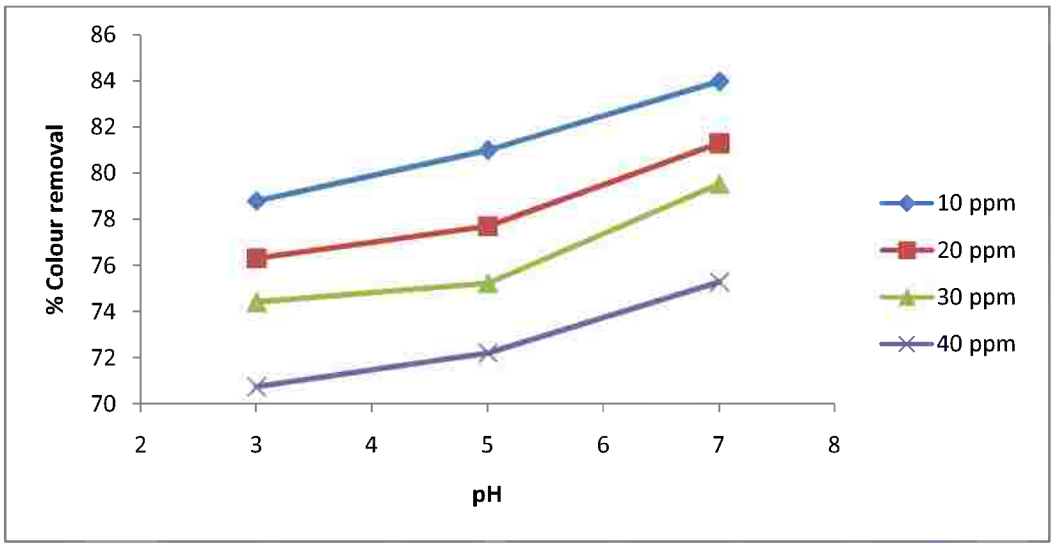

Figure 4.7: Effect of pH on the percentage colour removal of MB at different initial dye concentration (Catalyst loading = 0.5 g/l, air superficial velocity = 0.42 cm/s)

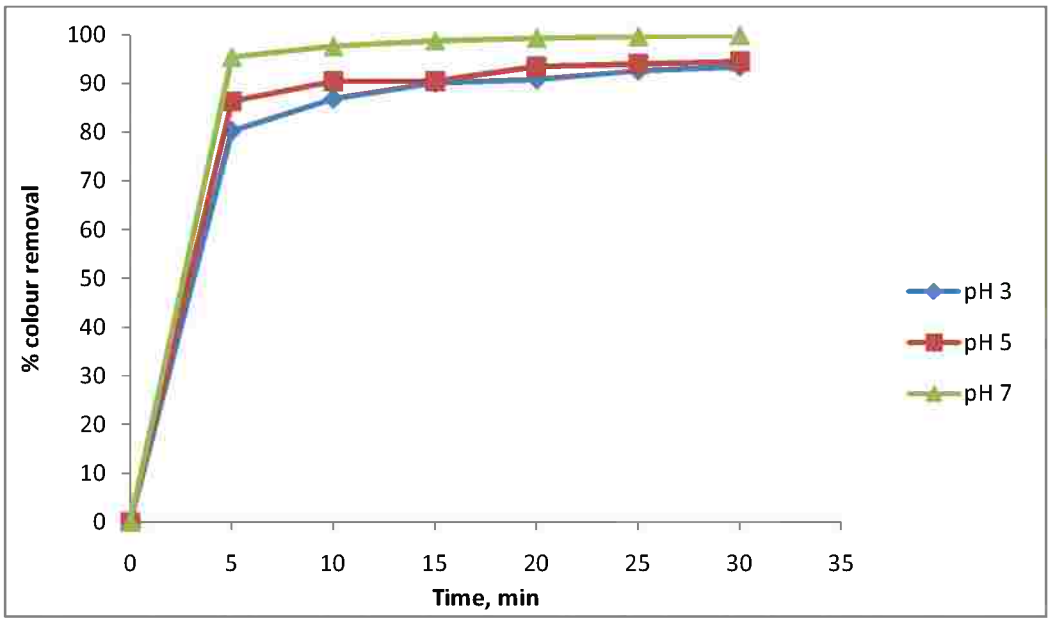

Figure 4.8: Effect of time on the percentage colour removal of MB at different initial solution pH
(Catalyst loading = 1 g/l, Ci = 10 ppm, air superficial velocity = 1.94 cm/s)

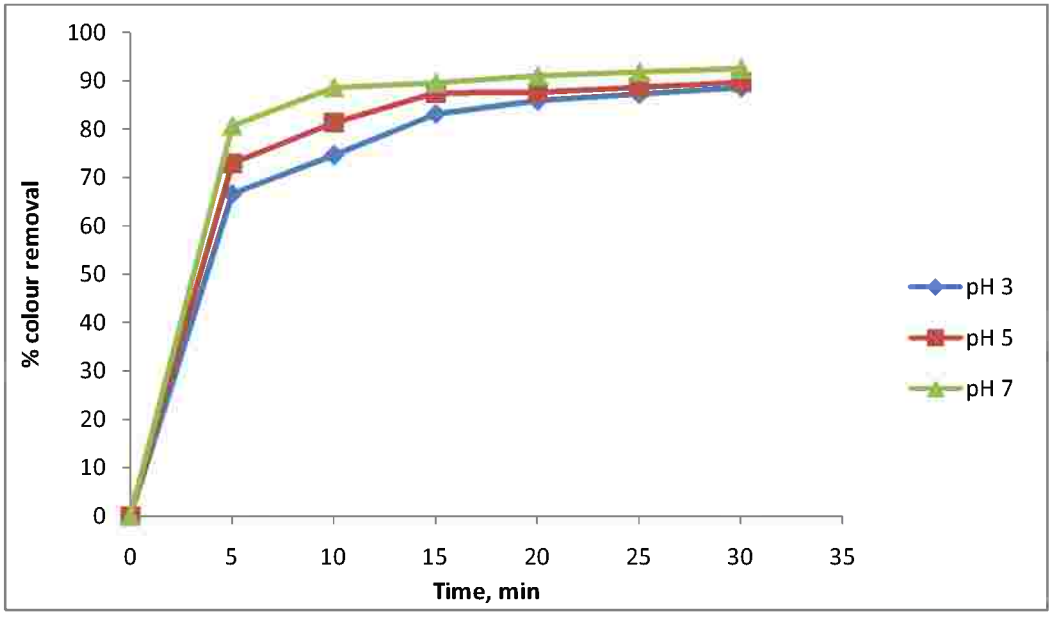

Figure 4.9: Effect of time on the percentage colour removal of MB at different initial solution pH
(Catalyst loading = 0.5g/l, C_i = 10 ppm, air superficial velocity = 1.94 cm/s)

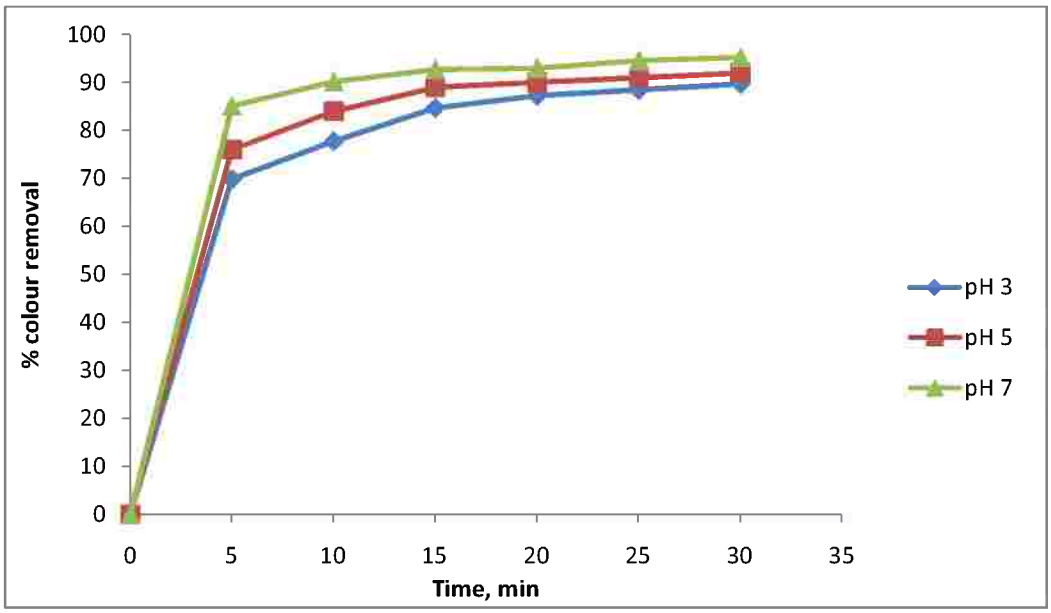

Figure 4.10: Effect of time on the percentage colour removal of MB at different initial solution pH
(Catalyst loading = 2 g/l, C_i = 10 ppm, air superficial velocity = 1.94 cm/s)

4.2.2. Effect of initial dye concentration

The influence of the initial dye concentration on the decolorization process was studied at broad range of dye concentration (10- 40 ppm). Figures (4.11 - 4.15) show that the percentage color removal was decreased with increasing of the initial dye concentration. This observation may be explained by: firstly, at high dye concentrations the generation of $OH^{\bullet}$ radicals on the surface of catalyst is reduced since the active sites are covered by dye ions. Secondly, with the increase in the dye concentration, less photons reach the photocatalyst surface (UV screening effect), resulting in slower production of hydroxyl radicals $OH^{\bullet}$. Consequently, the photocatalytic activity is decreased, since the fewer available $OH^{\bullet}$ radicals are required to oxidize more dye molecules. Thirdly, the interference of intermediates formed upon the degradation of Methylene Blue. Such competition would be more pronounced in the presence of a high concentration level of intermediates produced by the degradation of dye.[17, 109, 112, 113].

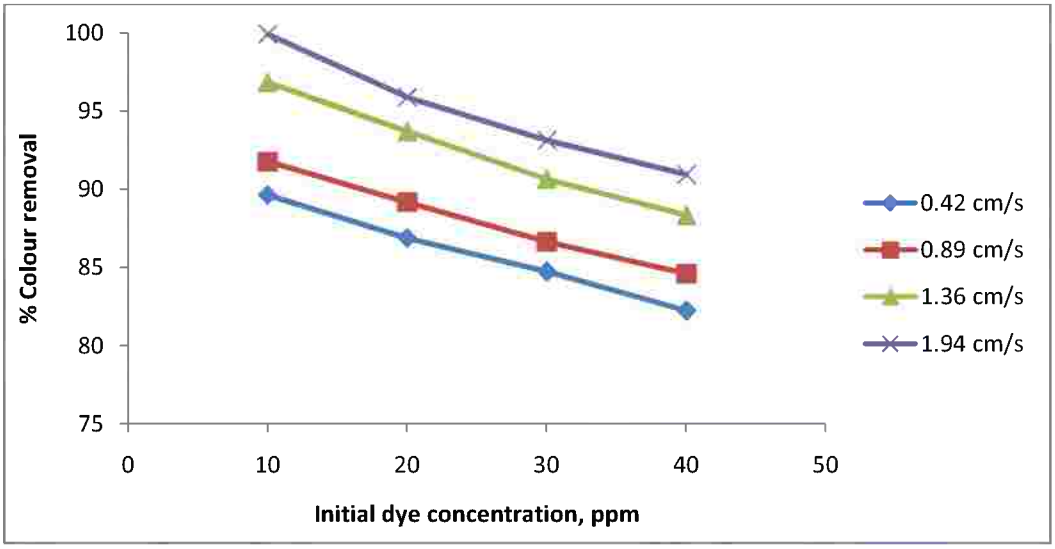

Figure 4.11: Effect of initial dye concentration on the percentage colour removal of MB at different air superficial velocity (Catalyst loading = 2 g/l, pH = 7)

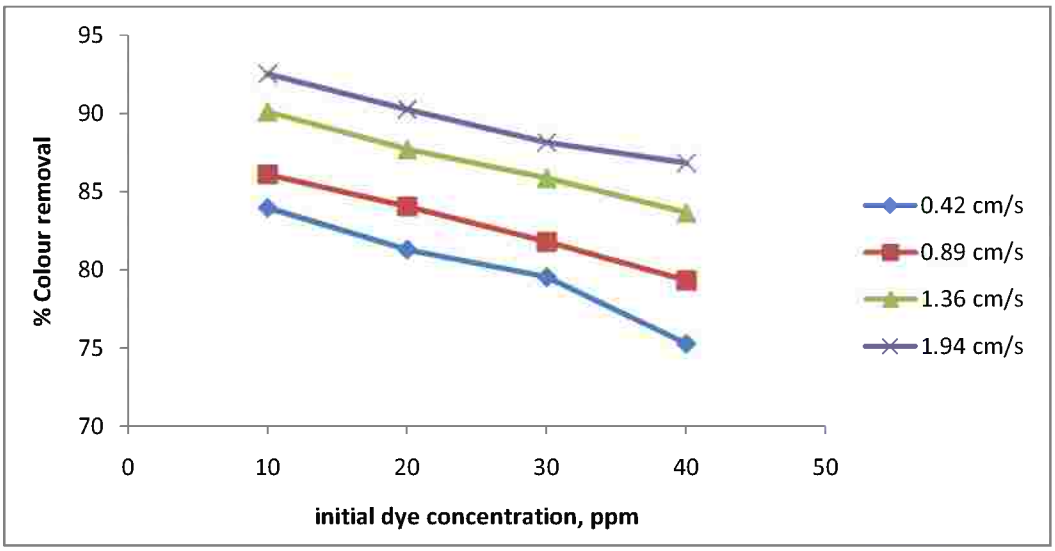

Figure 4.12: Effect of initial dye concentration on the percentage colour removal of MB at different air superficial velocity
(Catalyst loading = 0.5 g/l, pH = 7)

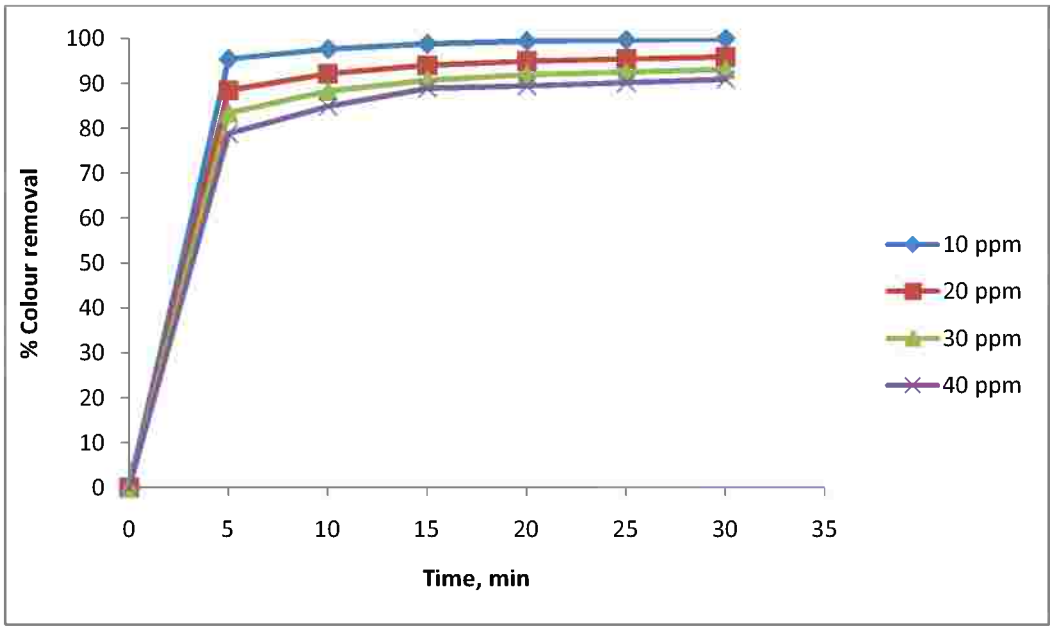

Figure 4.13: Effect of time on the percentage colour removal of MB at different initial dye concentration
(Catalyst loading = 1 g/l, pH = 7, air superficial velocity = 1.94 cm/s)

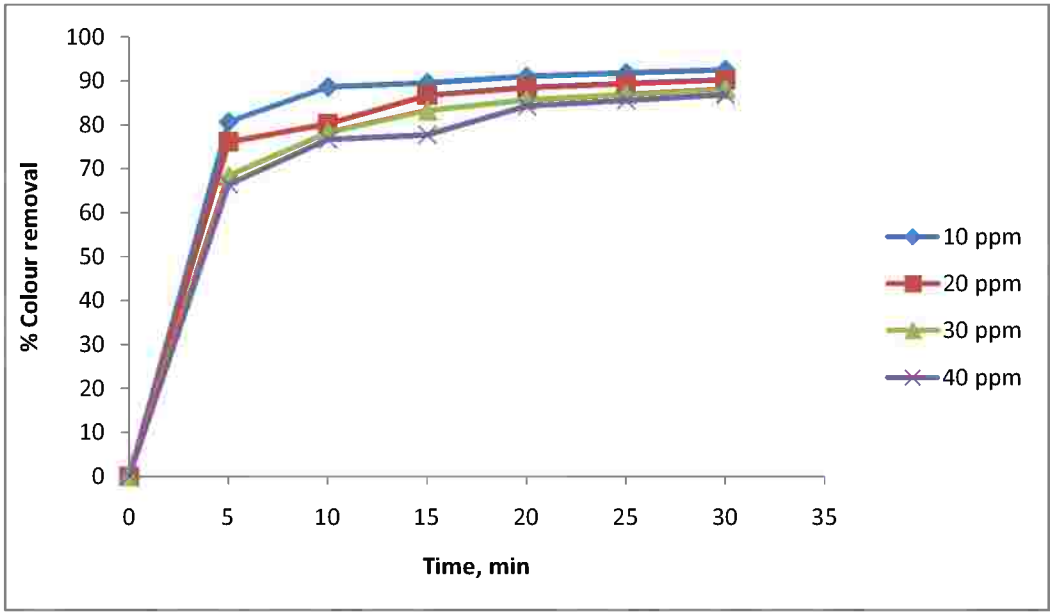

Figure 4.14: Effect of time on the percentage colour removal of MB at different initial dye concentration
(Catalyst loading = 0.5 g/l, pH = 7, air superficial velocity = 1.94 cm/s)

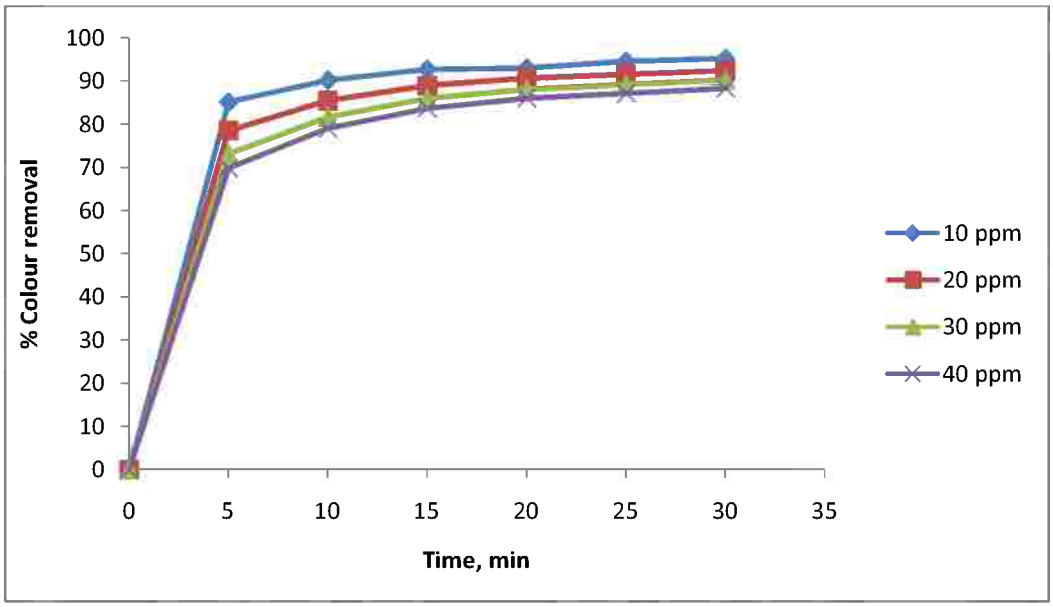

Figure 4.15: Effect of time on the percentage colour removal of MB at different initial dye concentration
(Catalyst loading = 2 g/l, pH = 7, air superficial velocity = 1.94 cm/s)

4.2.3. Effect of TiO_2 loading

Figures (4.16-4.20) show the effect of TiO_2 loading on the MB removal. it was found that the removal efficiency firstly increase gradually as the catalyst loading increases, then decreases with any further increases in the loading amount. This means that there is a limit of catalyst loading that must be used for the photodegradation of MB, above which, the rate of degradation decreases. This is in agreement with the previous studies [17, 109, 112, 113]. This may be attributed to the increase in the amount of catalyst resulting in increasing the number of active sites on the TiO_2 surface, which in turn increase the number of hydroxyl and superoxide radicals. when the concentration of the catalyst increases above specific value, the degradation rate decreases due to the scattering of the light by the suspension therefore, $OH^{\bullet}$ radical, a primary oxidant in the photocatalytic system decreased and the efficiency of the degradation reduced. Another reason is that the nanoparticles show a great tendency to aggregate due to high surface energy combined with their high surface area to volume ratio, so the increase of catalyst concentration beyond the optimum may result in the agglomeration of catalyst particles, hence a part of the catalyst surface become unavailable for photon absorption, consequently, degradation rate decrease.

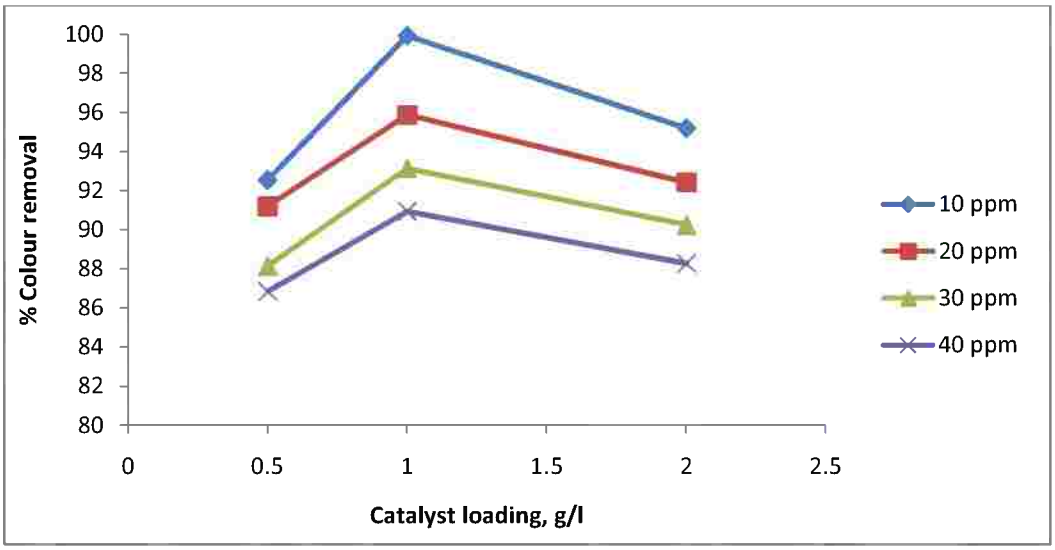

Figure 4.16: Effect of catalyst loading on the percentage colour removal of MB at different initial dye concentration
(pH = 7, air superficial velocity = 1.94 cm/s)

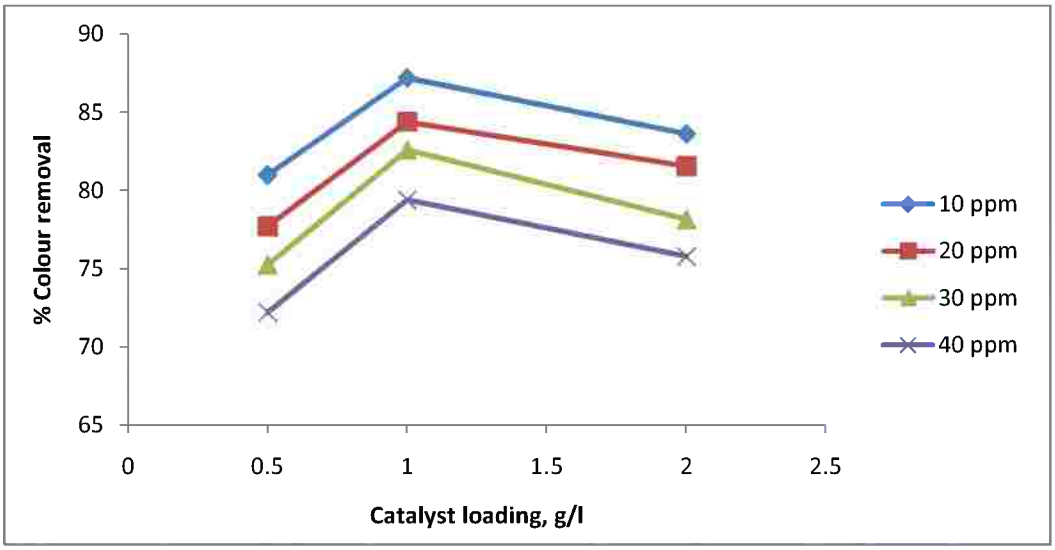

Figure 4.17: Effect of catalyst loading on the percentage colour removal of MB at different initial dye concentration
(pH = 5, air superficial velocity = 0.42 cm/s)

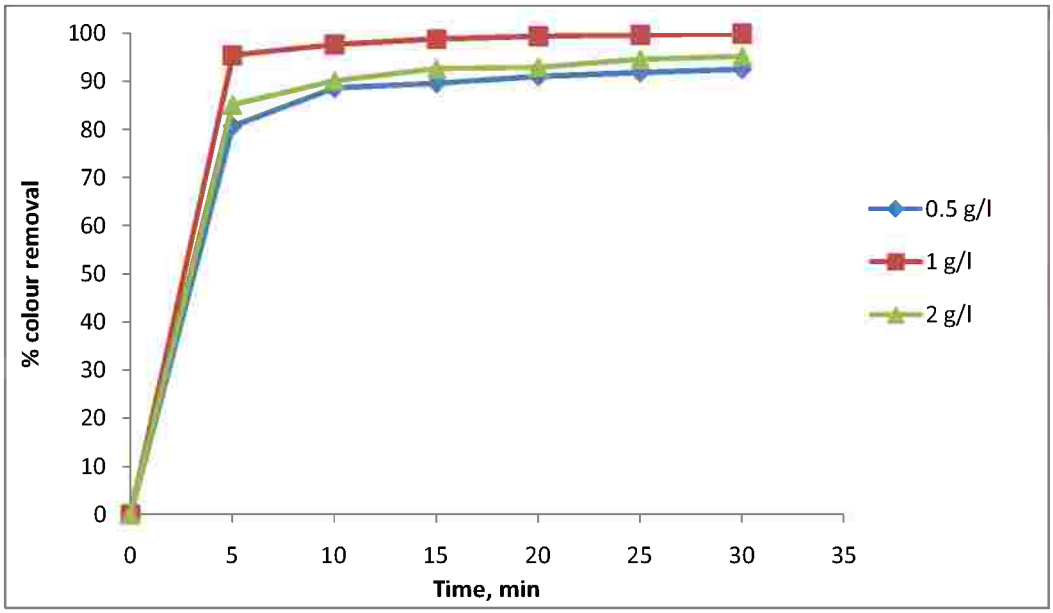

Figure 4.18: Effect of time on the percentage colour removal of MB at different of catalyst loading
(C_i= 10 ppm, pH = 7, air superficial velocity = 1.94 cm/s)

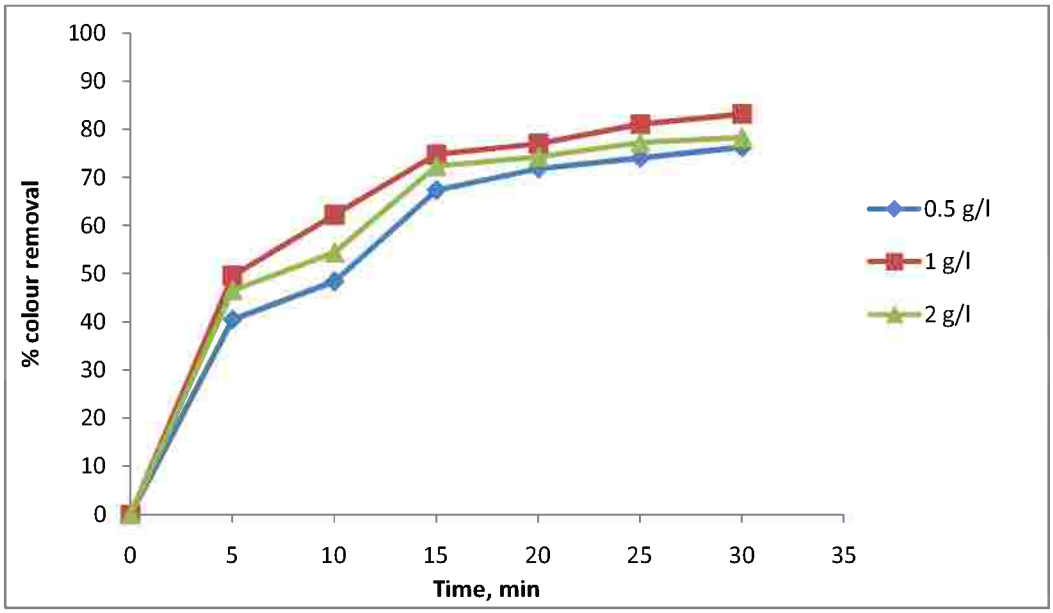

Figure 4.19: Effect of time on the percentage colour removal of MB at different of catalyst loading
(C_i= 20 ppm, pH = 3, air superficial velocity = 0.42 cm/s)

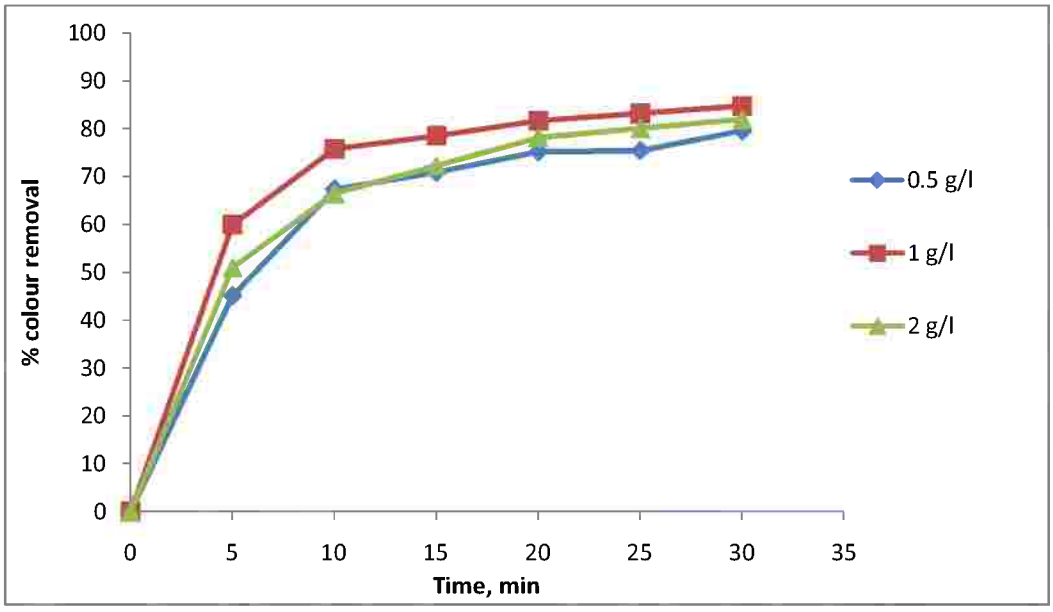

Figure 4.20: Effect of time on the percentage colour removal of MB at different of catalyst loading
(C_i= 30 ppm, pH = 7, air superficial velocity = 0.42 cm/s)

4.2.4. Effect of air superficial velocity

Figures (4.21-4.25) show the effect air superficial velocity on the degradation percentage of MB. It was found that as the air superficial velocity increases the percent degradation increases. This may be ascribed to that the increase in air superficial velocity leads to provide more oxygen to the system. Oxygen is responsible for scavenging the electrons generated by UV radiation which leading to production of more hydroxyl radical. The former can oxidize and destroy the dye molecule. Another reason is that increasing the air superficial velocity causes the TiO_2 particles to be more dispersed in the solution, hence exposed to more radiation. As well, increasing air superficial velocity enhance the mass transfer rate of dye molecule towards the titanium oxide surface through the diffusion layer [25].

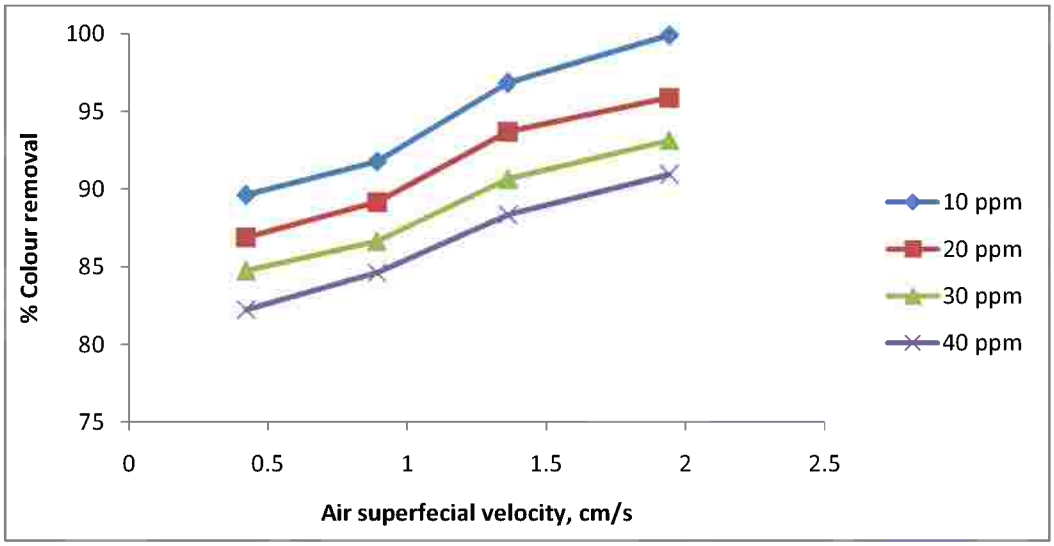

Figure 4.21: Effect of air superficial velocity on the percentage colour removal of MB at different initial dye concentration (Catalyst loading = 1 g/l, pH = 7)

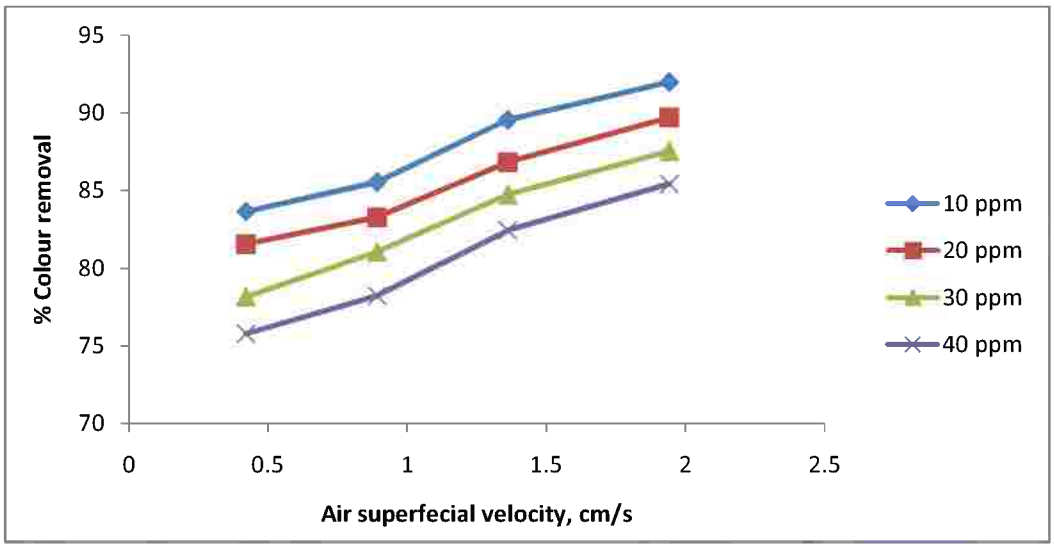

Figure 4.22: Effect of air superficial velocity on the percentage colour removal of MB at different initial dye concentration
(Catalyst loading = 2 g/l, pH = 5)

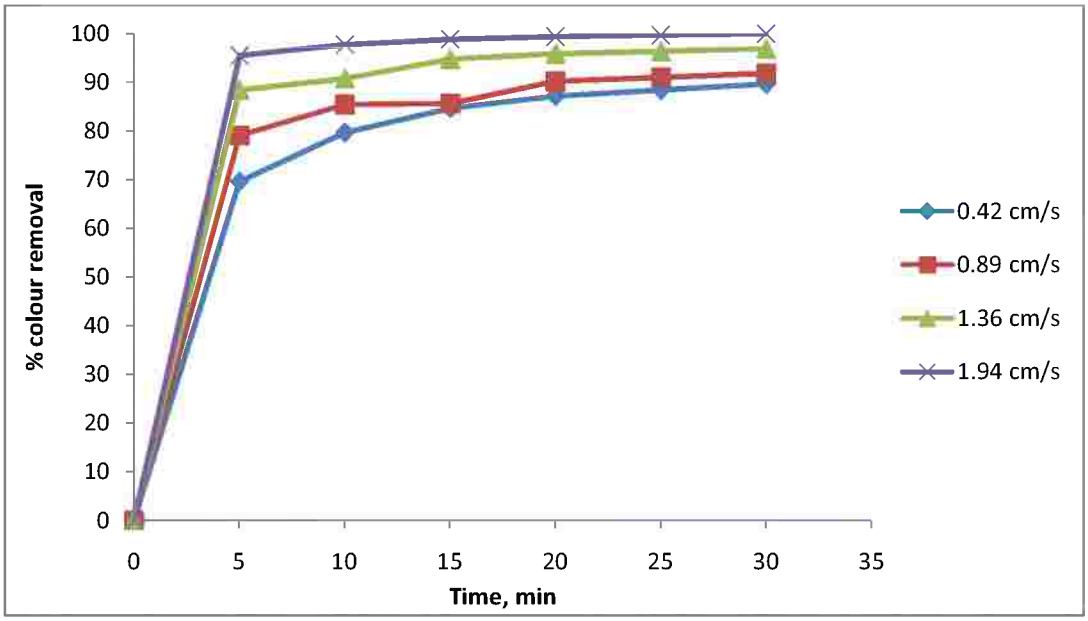

Figure 4.23: Effect of time on the percentage colour removal of MB at different air superficial velocity
(C_i= 10 ppm, pH = 7, catalyst loading = 1 g/l)

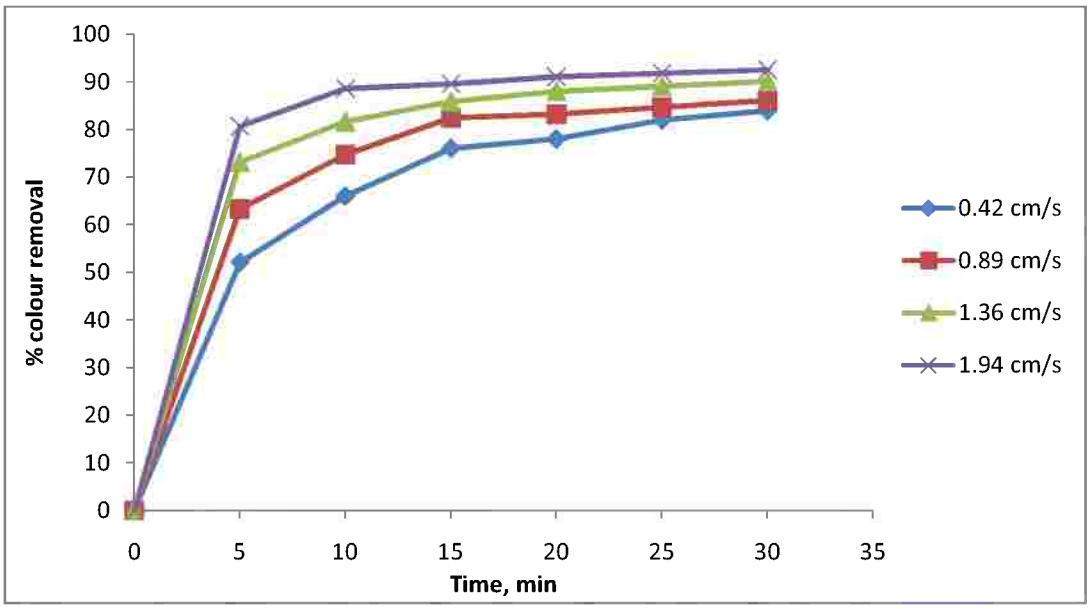

Figure 4.24: Effect of time on the percentage colour removal of MB at different air superficial velocity
(C_i= 10 ppm, pH = 7, catalyst loading = 0.5 g/l)

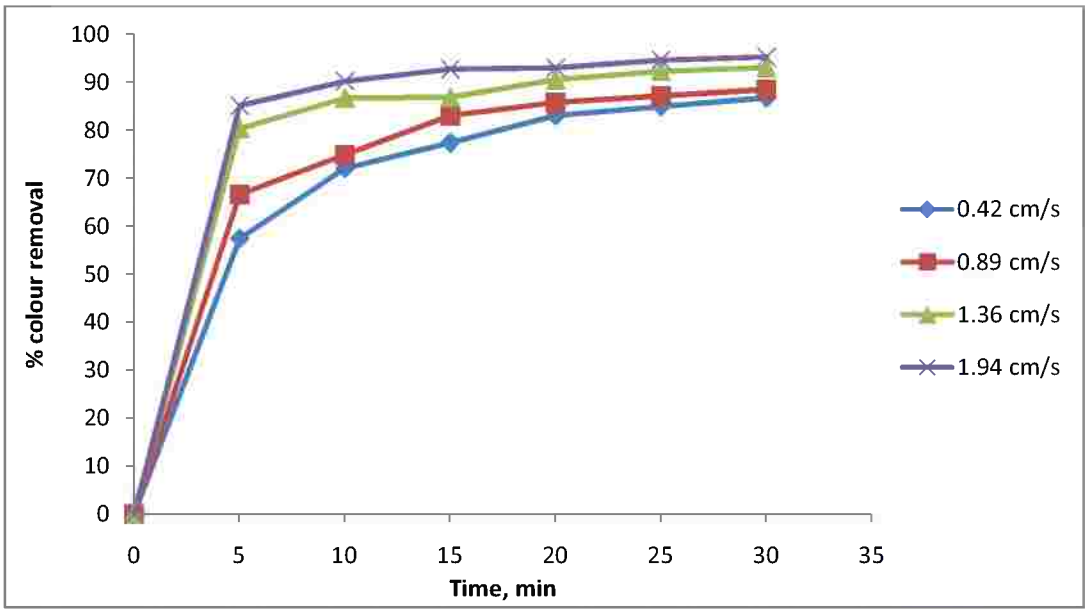

Figure 4.25: Effect of time on the percentage colour removal of MB at different air superficial velocity
(C_i= 10 ppm, pH = 7, catalyst loading = 2 g/l)

4.3 Performance of immobilized TiO_2 on glass chips on the degradation of methylene blue.

Slurry type reactors are commonly used where upon the photocatalyst particles have to be separated by filtration, coagulation, flocculation or centrifugation achieving a catalyst free solution and recycling the catalyst. These downstream processes are costly, which is a reasonable limitation of using a slurry reactor on an industrial scale. To avoid the separation step, the photocatalyst has to be fixed onto a support material.

In the present study, the nano particles titanium dioxide is immobilized on a glass chips by dip coating technique. To evaluate the performance of immobilized titanium dioxide, the decolorization of MB were carried out at air superficial velocity ranging from 0.42 to 1.94 cm/s , initial dye concentration of 40 ppm, catalyst loading of about 1 g/l and initial solution pH 7. (Cf. Figure 4.26).

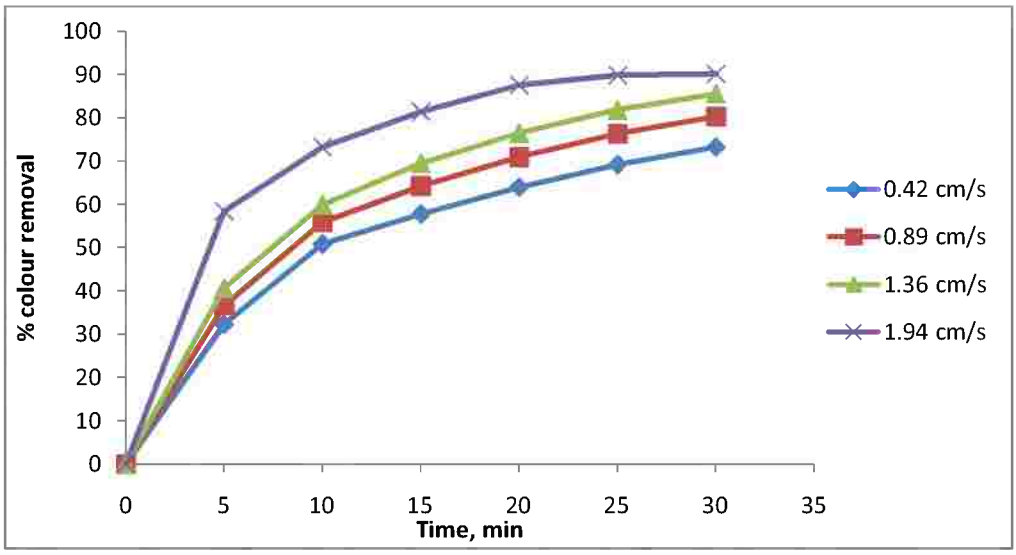

Figure 4.26: Effect of time on the percentage colour removal of MB using immobilized TiO_2 at different air superficial velocity (C_i= 10 ppm, pH = 7, catalyst loading ≈ 1 g/l)

Figure (4.27) show the performance of both slurry reactor and immobilized one. The results showed that the slurry reactor has higher photocatalytic activity than immobilized. This is may be attributed to the lower surface area of the immobilized catalyst that is exposed to the UV light [102].

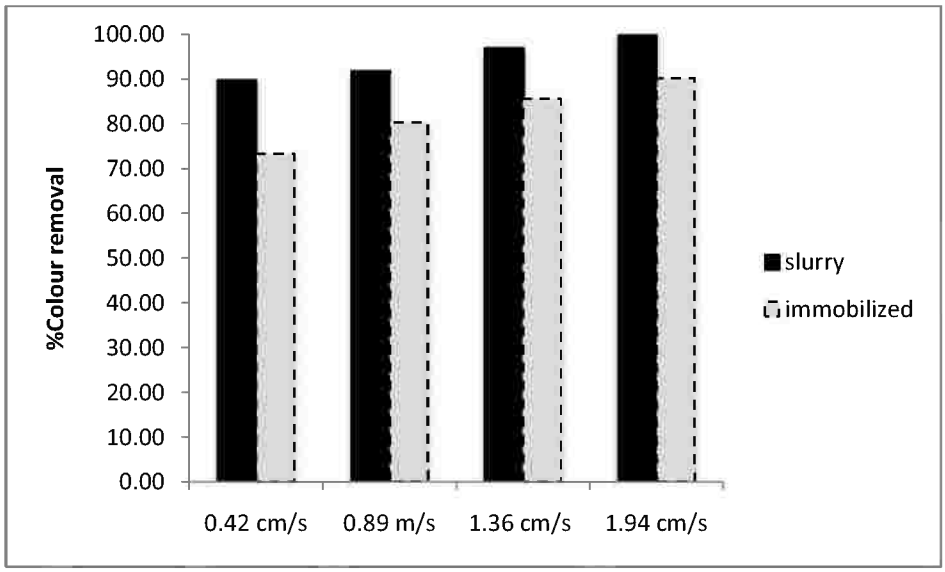

Figure 4.27: percentage colour removal of MB using slurry and immobilized TiO_2 at different air superficial velocity (C_i= 10 ppm, pH = 7, catalyst loading ≈ 1 g/l)

4.4. Kinetics of decolorization of Methylene blue on TiO_2[108]

4.4.1. Identification of the reaction order

4.4.1.1. Pseudo-first-order kinetic model (Lagergren's rate equation)

In this model, the kinetic rate in differential form and its analytical solution can be expressed as

$$\frac{dq_t}{dt} = k(q_e - q_t)$$

$$\log(q_e - q_t) = \log(q_e) - \frac{k}{2.303} t$$

Where q_e and q_t are the solid-phase concentration at equilibrium and at time (t), respectively. Here, k is the reaction rate constant in s^{-1}.

4.4.2.2. Pseudo second-order kinetic model

In this model, the kinetic rate in differential form and its analytical solution can be expressed as

$$\frac{dq_t}{dt} = k(q_e - q_t)^2$$

$$\frac{t}{q_t} = \frac{1}{kq_e^2} + \frac{1}{q_e} t$$

Where q_e and q_t are the solid-phase concentration at equilibrium and at time t, respectively. Here, the units of k are g/(mol s) provided that q is in mol/g.

The kinetic model for solid- liquid reactions was solved using the non-linear fitting and integration functions in Matlab.

Figures (4.28-4.30) show the order of heterogeneous reactions which is fit to pseudo first order reaction.

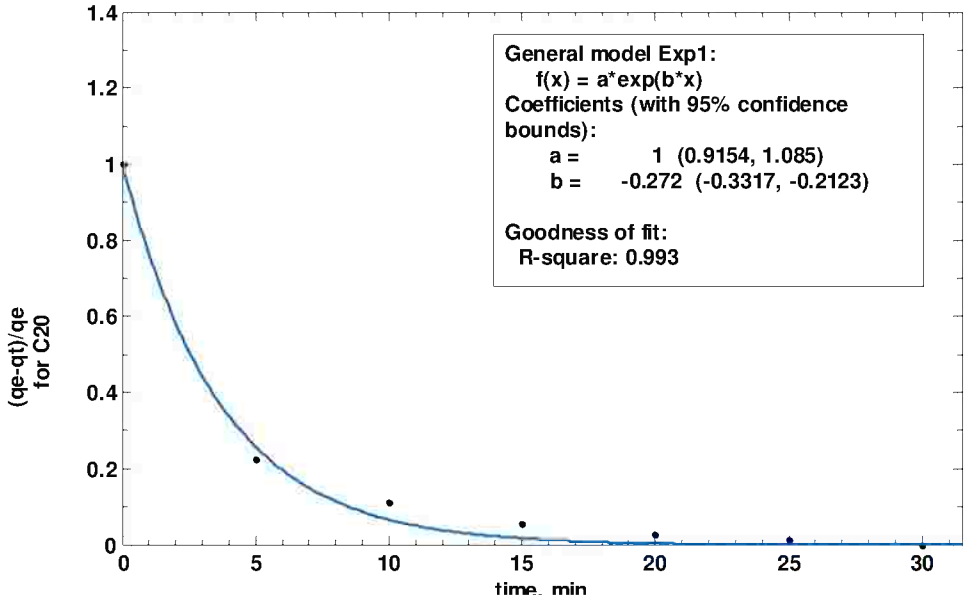

Figure 4.28: fitting of data to pseudo first order rate equation
(Air superficial velocity = 0.42 cm/s, C_i= 10 ppm, pH = 7, catalyst loading=1 g/l)

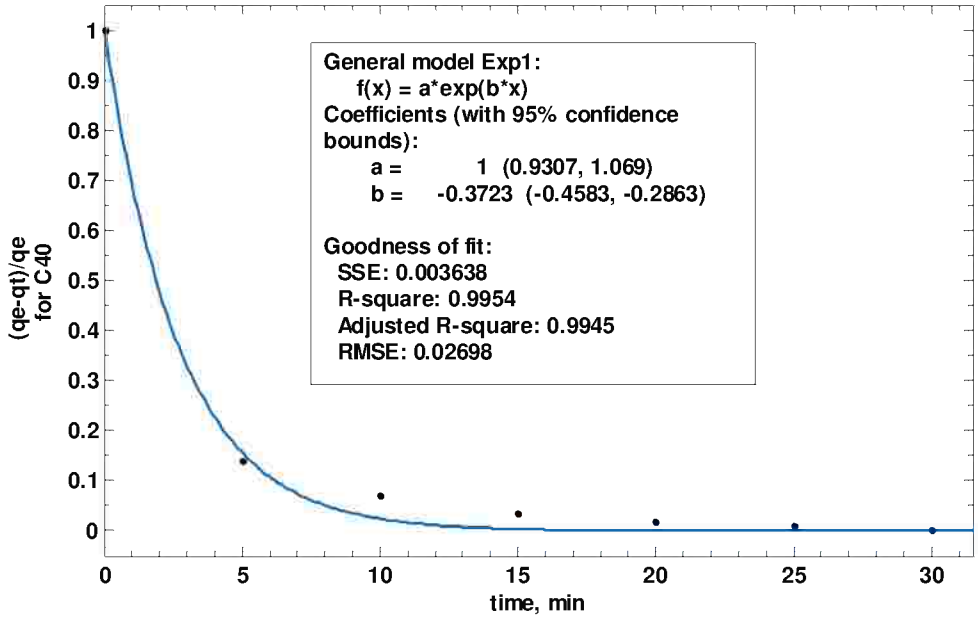

Figure 4.29: fitting of data to pseudo first order rate equation (Air superficial velocity = 0.89 cm/s, C_i= 10 ppm, pH = 7, catalyst loading=1 g/l)

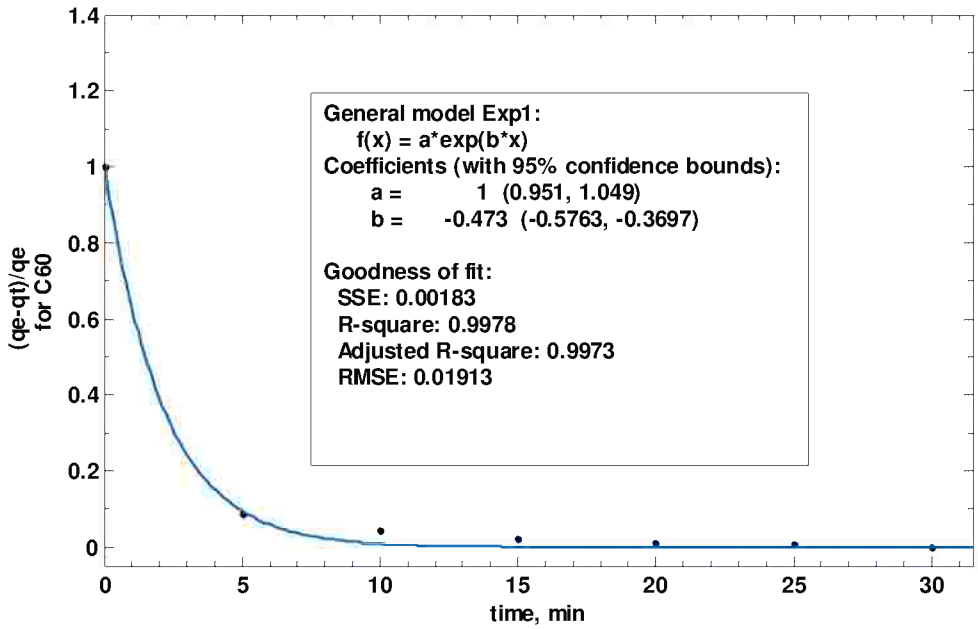

Figure 4.30: fitting of data to pseudo first order rate equation (Air superficial velocity = 0.89 cm/s, C_i= 10 ppm, pH = 7, catalyst loading=1 g/l)